• Review Article •

Differences of the lamina cribrosa between primary open angle glaucoma and non-pathologic high myopia

Qing-Qing Mu[1,2], *Ping Ge*[1,2], *Xu Liu*[1], *Jun Jia*[1], *Na Cui*[1], *Xiang-Xiang Yang*[1], *Rui-Xue Zhang*[1], *Yan Liu*[1,2], *Yuan-Yuan Zhang*[1,2], *Yuan He*[1,2]

[1]Department of Ophthalmology, the Second Affiliated Hospital of Xi'an Medical University, Xi'an 710038, Shaanxi Province, China
[2]Xi'an Medical University, Xi'an 710021, Shaanxi Province, China
Correspondence to: Yuan He. Xi'an Medical University; Department of Ophthalmology, The Second Affiliated Hospital of Xi'an Medical University, Xi'an 710038, Shaanxi Province, China. heyuan@xiyi.edu.cn
Received: 2025-06-13 Accepted: 2026-02-24

Abstract

● Primary open angle glaucoma (POAG) is a chronic, blinding ocular disorder characterized by progressive degeneration of retinal ganglion cells (RGCs). Its incidence and prevalence of blindness continue to increase with global population aging. Non-pathologic high myopia (HM) has been established as an independent risk factor for POAG, and the two conditions share similar structural changes in the lamina cribrosa (LC) during the early phase of optic nerve injury. This review summarizes the common and distinct pathological alterations of LC in POAG and HM, with the aim of clarifying its central role in the initiation and progression of optic nerve damage. Elucidating these similarities and differences may facilitate early detection and targeted intervention strategies for at-risk individuals from a structural perspective.

● **KEYWORDS:** non-pathologic high myopia; primary open angle glaucoma; optic disc; lamina cribrosa; retinal nerve fiber layer

DOI:10.18240/ijo.2026.06.19

Citation: Mu QQ, Ge P, Liu X, Jia J, Cui N, Yang XX, Zhang RX, Liu Y, Zhang YY, He Y. Differences of the lamina cribrosa between primary open angle glaucoma and non-pathologic high myopia. *Int J Ophthalmol* 2026;19(6):1177-1185

INTRODUCTION

Glaucoma is a multifactorial neurodegenerative disease of the optic nerve, characterized by the progressive loss of retinal ganglion cells (RGCs), and is the leading cause of irreversible blindness worldwide[1]. Primary open angle glaucoma (POAG), the most prevalent form, accounts for more than 70% of all glaucoma cases, with approximately 57.5 million individuals affected globally[2]. POAG typically progresses insidiously and is difficult to detect at an early stage. Many patients are already experiencing significant visual impairment at the time of diagnosis[3], and available treatment options remain limited, severely impacting quality of life. Therefore, opportunistic early screening of high-risk populations, such as intraocular pressure (IOP) measurement, visual field testing, and optical coherence tomography (OCT) imaging of the optic nerve, plays a crucial role in improving early detection rates[4-5]. Emerging evidence indicates that HM is an independent risk factor for POAG, with individuals with high myopia (HM) having approximately a sixfold increased risk of developing POAG compared to the general population[6]. The lamina cribrosa (LC) region at the optic nerve head (ONH) plays a central role in the onset and progression of glaucomatous optic nerve damage, and similar structural changes in the LC have also been observed in HM[7]. Therefore, a comparative analysis of LC structural characteristics in POAG and HM may contribute to the early identification of individuals at high risk and the development of targeted intervention strategies to reduce the burden of POAG-related vision loss[8].

This narrative review was based on a literature search of the PubMed, Web of Science, and Embase databases. The search keywords mainly included "lamina cribrosa", "primary open-angle glaucoma", "non-pathologic high myopia", and "optic nerve head", with a focus on English-language articles published in the past 10y. Original research articles, reviews, and clinical studies were primarily included, with particular attention to studies investigating LC morphology and its imaging assessment, in order to compare the structural differences of the LC between POAG and HM.

EPIDEMIOLOGICAL ANALYSIS

With changes in modern lifestyles and visual habits, HM has become a major global public health concern[9]. Because the posterior segment alterations associated with HM

share similarities with glaucomatous optic nerve damage, distinguishing HM-related changes from glaucoma has become increasingly challenging, drawing growing attention from ophthalmologists worldwide[10-11]. Epidemiological studies estimate that the global population affected by HM will increase dramatically, from approximately 163 million individuals in 2000 to nearly 938 million by 2050[12]. East Asia shows a particularly high prevalence of myopia among children and adolescents, far exceeding that reported in Western and less economically developed regions[13]. In China, recent national surveillance data indicate that more than half of children and adolescents are myopic, with the prevalence of HM increasing markedly with age[14]. HM is associated with multiple sight-threatening complications, including retinal detachment, choroidal neovascularization, and glaucoma[15]. Accumulating evidence from cross-sectional studies, longitudinal cohorts, and Meta-analyses consistently demonstrates that myopia is an independent risk factor for POAG[16], with a clear dose-response relationship. The risk of POAG increases significantly with higher degrees of myopia and longer axial length, particularly in eyes exceeding -6.0 diopters or an axial length of approximately 26.5 mm[17]. Overall, with the continued global rise in HM prevalence, the burden of POAG comorbidity is expected to increase correspondingly, making this an emerging clinical and public health challenge.

Anatomy of the Lamina Cribrosa and Imaging Assessment

Lamina cribrosa anatomy and biomechanical characteristics The LC is located in the deep portion of the ONH and serves as the primary structural support for RGC axons as they pass through the posterior pole of the eye, while simultaneously bearing bidirectional forces from IOP and cerebrospinal fluid pressure (Figure 1)[18]. The LC is primarily composed of multiple layers of laminar beams and the laminar pores they form (Figure 2)[19]. These beams are mainly constituted of collagen fibers, elastic fibers, and a proteoglycan-rich extracellular matrix (ECM), providing mechanical support to the axons and participating in local metabolic and microcirculatory maintenance[20-21]. Under normal conditions, the LC exhibits a slight posterior curvature, the degree of which is influenced by scleral stiffness[22-23], IOP levels[21] and the supportive status of adjacent ocular structures[24]. When IOP is elevated or axial length is increased, the LC may undergo posterior displacement, thinning, or pore enlargement, leading to axonal compression, impaired perfusion, and RGC injury[25].

Common imaging techniques for lamina cribrosa assessment With advances in OCT, the LC can now be directly imaged *in vivo* and quantitatively analyzed. The two main OCT modalities used in research and clinical practice

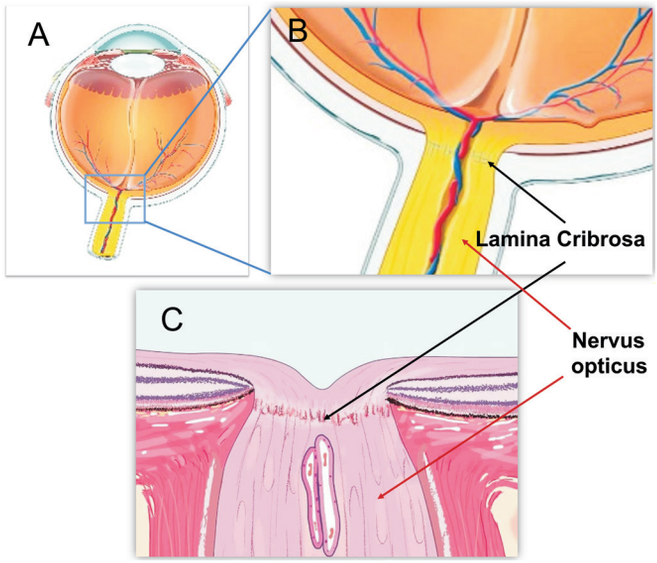

Figure 1 Schematic illustration of the location and structure of the lamina cribrosa (LC)[18] A: Schematic diagram of the whole eyeball, with the optic nerve head region highlighted by the blue box; B: Magnified view of the optic nerve head, showing that the lamina cribrosa is located within the scleral canal and serves as a key structure through which retinal ganglion cell axons and the central retinal artery and vein pass; C: Histological schematic illustration of the lamina cribrosa.

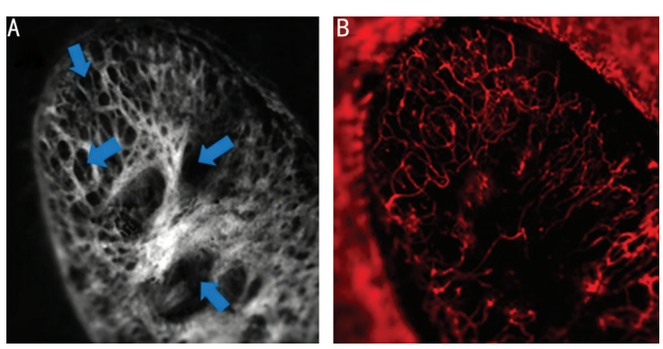

Figure 2 Representative array confocal images of the lamina cribrosa microstructure and microvasculature after removal of prelaminar tissue[19] A: Structured light array confocal image showing the lamina cribrosa beams (gray) and laminar pores (blue arrows); B: Structured light fluorescence array confocal image demonstrating DiI-labeled vessels within the lamina cribrosa, pseudo-colored in red.

are enhanced-depth imaging OCT (EDI-OCT) and swept-source OCT (SS-OCT). EDI-OCT improves visualization of deep tissues and is widely available[26], while SS-OCT offers deeper scanning and more complete visualization of the LC, particularly in highly myopic eyes or eyes with posterior scleral staphyloma[27]. Variations in imaging algorithms and measurement definitions across devices may affect comparability between studies[27-28].

Quantitative parameters of lamina cribrosa and their clinical significance The morphology of the LC can be objectively assessed using various quantitative parameters.

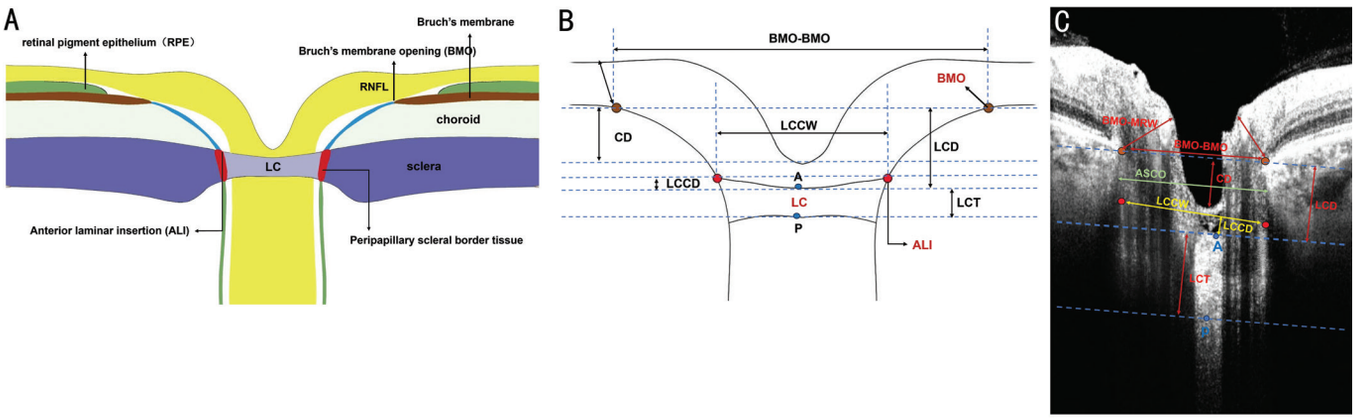

Figure 3 Schematic illustration of lamina cribrosa parameter measurements A: Anatomical illustration of the structures surrounding the lamina cribrosa; B: Theoretical schematic of lamina cribrosa parameters; C: Actual OCTA measurement example. In B and C, point A indicates the lowest point on the anterior surface of the LC, and point P indicates the lowest point on the posterior surface of the LC. The orange dots represent the BMO, and the red dots represent the ALI. BMO: Bruch's membrane opening; ALI: Anterior laminar insertion; LC: Lamina cribrosa; CD: Cup depth; LCT: Lamina cribrosa thickness; LCD: Lamina cribrosa depth; LCCD: Lamina cribrosa curve depth; LCCW: Lamina cribrosa curve width; BMO-MRW: Bruch's membrane opening-minimum rim width; BMO-BMO: Bruch's membrane opening diameter; ASCO: Anterior scleral canal opening reference line; RNFL: Retinal nerve fiber layer.

Commonly used metrics include, Bruch's membrane opening (BMO) diameter, Bruch's membrane opening-minimum rim width (BMO-MRW), minimum rim area (MRA), lamina cribrosa thickness (LCT), lamina cribrosa depth (LCD), lamina cribrosa curvature index (LCCI), and the relative displacement between the anterior scleral canal opening and BMO (ASCO/BMO offset; Figure 3). LCT represents the vertical distance between the anterior and posterior surfaces of the LC, reflecting its mechanical support capacity, although measurements may be limited when the posterior boundary is not visible[29-30]. LCD is defined as the vertical distance from the anterior LC surface to the BMO plane, which evaluates the posterior bowing of the LC, and its accuracy depends on precise identification of the BMO[31-32]. LCCI quantifies the overall posterior bowing of the LC and is calculated as LCCI=(LCCD/LCCW)×100[33], where lamina cribrosa curve depth (LCCD) is the vertical distance from the deepest point of the anterior LC surface to the reference line connecting the two anterior laminar insertion points, and lamina cribrosa curve width (LCCW) is the length of this reference line[34-35]. Compared with LCD, LCCI better reflects the overall curvature of the LC and is more useful for distinguishing glaucomatous posterior bowing from myopia-related tractional deformation[30,36]. BMO-MRW and MRA represent the shortest distance or area from the BMO to the nearest retinal nerve fiber layer boundary, reflecting axonal loss and the integrity of the ONH[37]. ASCO/BMO offset indicates the positional displacement of the anterior scleral canal opening relative to the BMO and assesses three-dimensional remodeling of the ONH[38]. No single parameter can comprehensively capture the complex structural changes of the LC; therefore, clinical and research assessments typically recommend a combined analysis of LCT, LCD, LCCI, BMO-MRW/MRA, and ASCO/BMO offset to provide a more complete and clinically meaningful evaluation. Table 1 summarizes the definitions, measurement methods, and clinical significance of these commonly used parameters.

Lamina Cribrosa Remodeling in POAG The LC remodeling in POAG exhibits clear stage-dependent progressive changes, rather than simple uniform structural damage[20]. Based on quantitative analyses using EDI-OCT or SS-OCT, the structural evolution of the LC can be categorized into three relatively continuous stages: early, middle, and late. 1) Early stage: In the initial phase of POAG, elevated IOP and local biomechanical stress first induce structural responses in the LC[30,39]. Large-scale clinical imaging studies have demonstrated that LCT decreases from approximately 290 μm in normal controls to around 257 μm in early POAG[1]. Some patients also exhibit focal laminar pore enlargement, disorganized laminar beams, or subtle posterior displacement; these microscopic changes may precede optic disc cupping and visual field defects, suggesting their potential value for early prediction[30,40]. At this stage, LC structure retains a certain degree of plasticity, primarily reflecting its initial response to mechanical stress. 2) Middle stage: With disease progression, posterior displacement and bowing of the LC become more pronounced[34]. Using EDI-OCT, the mean LCD in mild-to-moderate POAG patients was measured at approximately 448 μm, significantly deeper than in the early stage (≈390 μm)[41]. Concurrently, the LCCI calculated from OCT images were significantly higher in middle-stage POAG compared with normal eyes[42]. These structural alterations show a high degree of spatial concordance with sectoral thinning of the retinal nerve fiber layer (RNFL) and

Table 1 Quantitative lamina cribrosa parameters and their clinical significance

Parameters	Definition	Clinical significance
LCT	Vertical distance between the anterior and posterior surfaces of the lamina cribrosa	Reflects mechanical support capacity; may be limited if posterior boundary is unclear
LCD	Vertical distance from the anterior LC surface to the BMO plane	Evaluates posterior bowing of the LC; accuracy depends on precise BMO identification
LCCI	LCCI=(LCCD/LCCW)×100; LCCD is the vertical distance from the deepest point of anterior LC surface to the line connecting anterior laminar insertion points (LCCW)	Quantifies overall posterior bowing; better reflects curvature than LCD; distinguishes glaucomatous from myopia-related deformation
BMO-MRW/MRA	Shortest distance or area from BMO to the nearest retinal nerve fiber layer boundary	Reflects axonal loss and optic nerve head integrity
ASCO/BMO offset	Positional displacement of the anterior scleral canal opening relative to BMO	Assesses 3D remodeling of the optic nerve head

LCT: Lamina cribrosa thickness; LCD: Lamina cribrosa depth; LCCI: Lamina Cribrosa Curvature Index; BMO: Bruch's membrane opening; BMO-MRW: Bruch's membrane opening-minimum rim width; MRA: Minimum rim area; LCCW: Lamina cribrosa curve width; LCCD: Lamina cribrosa curve depth; ASCO: Anterior scleral canal opening; BMO offset: Bruch's membrane opening offset; LC: Lamina cribrosa.

ganglion cell-inner plexiform layer (GC-IPL)[35-36], suggesting a close relationship between mechanical strain-induced LC remodeling and RGC axonal injury[30]. 3) Late stage: In advanced POAG, the LC exhibits pronounced morphological reconstruction[43]. Studies have reported a marked reduction in central LCT in POAG patients, often averaging below 250 μm with considerable interindividual variability, showing significant differences compared to healthy controls[29,44]. The posterior deformation of the LC becomes more pronounced, with some eyes demonstrating frank posterior herniation or an inverted-arch configuration, changes that correspond to further increases in LCCI[38]. These irreversible forms of remodeling reflect substantial ECM reorganization and increased tissue stiffness, and may be accompanied by astrocyte activation and upregulation of inflammatory mediators such as tumor necrosis factor (TNF)-α, thereby exacerbating biomechanical stress and damage to RGCs[45].

Lamina Cribrosa Changes in High Myopia

Typical structural signs Patients with HM commonly exhibit optic disc tilt and torsion accompanied by peripapillary atrophy (PPA), forming characteristic arcuate zones that include the α-, β-, γ-, and δ-zones. The α-zone corresponds to mild pigmentary irregularities, the β-zone represents choroidal atrophy, the γ-zone denotes the region around the optic disc lacking BMO, and the δ-zone reflects deep posterior scleral alterations associated with HM (Figure 4)[23]. OCT and SS-OCT enable quantitative evaluation of these regions-including measurements such as BMO-MRW, peripapillary atrophic zone width, and choroidal thickness-thereby providing a structural basis for understanding the morphology of the ONH[46]. In addition, highly myopic eyes frequently present with characteristic ONH-related abnormalities such as posterior bowing of the perineural scleral canal and peripapillary hyperreflective ovoid mass-like structures (PHOMS), both of which can be clearly visualized on OCT and have been shown to correlate with the degree of axial elongation[47-48].

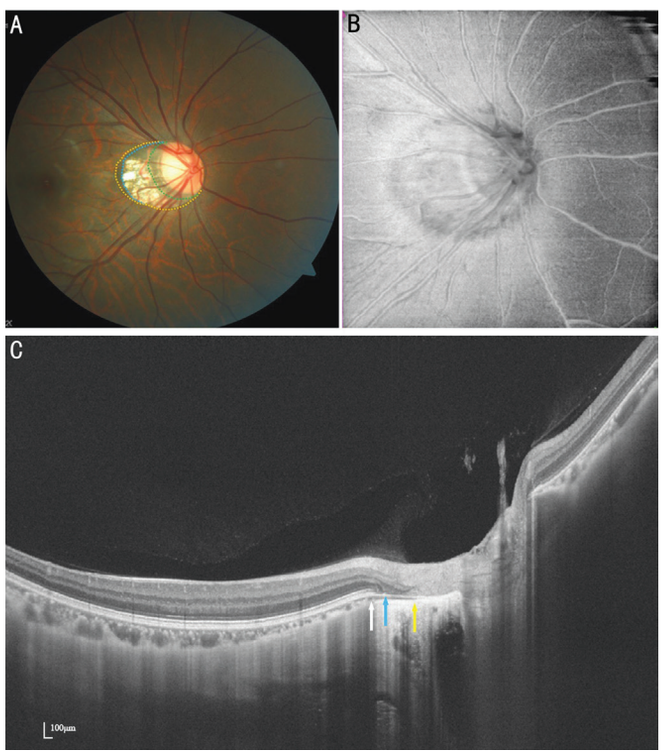

Figure 4 Multimodal imaging of PPA[23] Optic disk photograph (A) and *en face* image (B) show a myopic crescent temporally. Peripapillary alpha zone (yellow dots) appears as a hyperpigmentation zone. Peripapillary beta zone and gamma zone (blue dots) are characterized by a whitish area at the temporal optic disk border with underlying visible sclera and choroidal vessels. Delta zone (green dots) appears darker than the surrounding gamma zone. OCT imaging (C) demonstrates the borders of beta, gamma, and delta zone at the ends of RPE (white arrow), BMO (blue arrow), and the end of the scleral flange (yellow arrow). PPA: Peripapillary atrophy; OCT: Optical coherence tomography; RPE: Retinal pigment epithelium; BMO: Bruch's membrane opening.

Biomechanical alterations of the lamina cribrosa In HM, posterior pole stretching caused by axial elongation is the primary driver of LC remodeling, producing a pattern of change that differs markedly from that seen in POAG. In

Table 2 Comparison of lamina cribrosa structural changes between POAG and non-pathologic high myopia for clinical differentiation

Parameters	POAG	Non-pathologic high myopia
LCT	Marked thinning↓↓↓	Mild thinning↓
LCD	Pronounced posterior displacement↓↓↓	Minimal or negligible posterior displacement↓
LCCI	Persistently increased with a unidirectional posterior bowing	Variable changes, potentially influenced by axial elongation, LC tilt, or optic disc torsion
BMO-MRW	Reduced	Marked regional variation, with relatively narrower temporal and wider nasal sectors
ASCO/BMO offset	Not pronounced	Marked, predominantly directed superonasally
Focal lamina cribrosa defect	Relatively common	Occasionally observed, but with low frequency
RNFL	Segmental thinning with progressive damage	Largely preserved, with slow and localized damage
Lamina cribrosa remodeling mechanism	Mechanical compression and ECM remodeling	Posterior pole traction and adaptive remodeling

LCT: Lamina cribrosa thickness; LCD: Lamina cribrosa depth; LCCI: Lamina Cribrosa Curvature Index; BMO: Bruch's membrane opening; BMO-MRW: Bruch's membrane opening-minimum rim width; MRA: Minimum rim area; ASCO: Anterior scleral canal opening; BMO offset: Bruch's membrane opening offset; RNFL: Retinal nerve fiber layer; POAG: Primary open angle glaucoma; ECM: Extracellular matrix; LC: Lamina cribrosa.

highly myopic eyes, LCT typically shows only mild thinning, reflecting a global reduction induced by tensile stretching rather than the progressive and regionally pronounced thinning associated with elevated IOP and ECM remodeling in glaucoma. Similarly, the degree of LC posterior displacement in HM is generally small and may even approximate the normal range[27], further supporting the concept that highly myopic LC experience predominantly horizontal tensile forces instead of the characteristic posteriorly directed compressive load observed in POAG. In POAG, the LCCI usually shows a clear and sustained increase. For example, Kim *et al*[49] reported that the mean LCCI in POAG eyes (85.8±34.1 μm) was significantly higher than in healthy controls (68.2±32.3 μm, $P<0.001$). In contrast, the behavior of LCCI in high myopia is more variable and uncertain. Its fluctuations may be influenced by LC tilting secondary to axial elongation, as demonstrated by the Beijing Eye Study, which reported a mean LC tilt of 4.38° in highly myopic eyes compared with 0.04° in non-myopic eyes ($P<0.001$)[27], and may also relate to optic disc torsion or differences in scleral compliance[50]. In a prospective cohort study, Dai *et al*[51] found that highly myopic eyes exhibited significantly larger BMO areas (3.0 *vs* 2.3 mm^2, $P<0.001$) and anterior scleral canal opening (ASCO) areas (3.0 mm^2 *vs* 2.3 mm^2, $P<0.001$), accompanied by a markedly greater ASCO-BMO offset (median ≈376.1 μm compared with approximately 161.5 μm in POAG, $P<0.001$). The offset direction was predominantly superonasal. This traction-related remodeling produces substantial angulation of the neural canal[52], and may exert slow, localized effects on RGCs, rather than the widespread injury caused by mechanical compression typical of glaucoma[53]. It is noteworthy that focal LC defects can also occur in HM, although they are less frequent than in POAG. Enlargement of the BMO and LC bending, however, are common features shared by both conditions[23]. Based on OCT-derived quantitative metrics, LC remodeling in isolated HM is mainly characterized by LCT thinning, relatively increased BMO-MRW, and localized LC bending or stretching. These parameters provide valuable guidance for assessing ONH morphology in HM individuals and may aid in the early identification of those at risk of developing concomitant glaucoma (Table 2).

Clinical Value and Limitations of Lamina Cribrosa Assessment Quantitative assessment of LC structure demonstrates significant clinical value in the early diagnosis of POAG. Specifically, LCT is significantly lower in highly myopic eyes with POAG compared to eyes with simple HM. Chen *et al*[54] reported that when LCT falls below the threshold of ≤128 μm, the area under the receiver operating characteristic (ROC) curve for distinguishing the two conditions reaches 0.964, outperforming global RNFL thickness and vertical cup-to-disc ratio (C/D). LCD and LCCI reflect compressive posterior bowing deformation in POAG, whereas in HM, they primarily indicate traction-related morphological remodeling. These distinctions can aid in differentiating compressive-type from traction-type lesions[27,55]. Combined analysis of BMO-MRW and ASCO/BMO spatial offset can reveal geometric reconstruction of the ONH in highly myopic eyes, providing valuable insight into the origin of structural remodeling[38]. Meanwhile, BMO-based C/D offers a more stable assessment of C/D, particularly in eyes with enlarged or tilted optic discs associated with HM, reducing interference from pseudo C/D enlargement and thereby improving the sensitivity of glaucoma screening[56]. Optical coherence tomography angiography (OCTA) demonstrates that microvascular perfusion of the LC is significantly reduced in POAG, whereas in HM, vascular changes are mainly related to axial elongation and traction[56-57]. Focal LC defects may indicate localized RGC damage, further reflecting early functional risk[58].

However, there remain limitations in the clinical application of quantitative LC assessment. Small or markedly tilted optic

discs may result in incomplete imaging signals, affecting measurement accuracy[59]. In highly myopic eyes, axial elongation can alter image scaling and reduce signal quality in deeper structures, thereby decreasing LC visibility and measurement stability and increasing quantitative errors[60-61]. In addition, the lack of standardized protocols across different OCT or SS-OCT devices and algorithms limits multicenter comparisons and broader clinical implementation[62]. Therefore, LC structural parameters should be interpreted in conjunction with axial length, optic disc geometry, and other structural indicators to maximize their clinical utility in early POAG diagnosis and risk assessment for glaucoma in highly myopic eyes.

CONCLUSION AND PERSPECTIVES

The LC, as the critical structure through which RGC axons exit the eye, plays a central role in the pathogenesis and progression of glaucoma. In recent years, advances in OCT technology have enabled increasingly detailed visualization of the LC and its surrounding microenvironment. Morphological parameters such as LCT and posterior displacement have gradually transitioned from basic research to clinical quantification, allowing a more precise understanding of the overlapping yet distinct pathological mechanisms between POAG and HM. Overall, POAG is predominantly characterized by compressive posterior bowing of the LC, whereas HM is mainly driven by axial elongation and posterior scleral traction. Accumulating evidence indicates that LC posterior displacement, thinning, focal defects, and related structural alterations in POAG are closely associated with IOP-related biomechanical stress. In contrast, LC tilt, BMO/ASCO offset, and optic disc torsion observed in HM primarily reflect long-term traction-induced structural remodeling.

Although the LC phenotypes of these two conditions partially overlap, LC-related parameters, such as lamina LCD, LCCI, BBMO-MRW, and ASCO/BMO offset, provide novel quantitative metrics for distinguishing “glaucomatous” from “high-myopic” structural changes. This distinction has important clinical implications. For instance, in highly myopic eyes, LC morphological alterations driven predominantly by axial elongation, and traction do not necessarily indicate the need for aggressive IOP-lowering therapy. In contrast, the concomitant presence of pronounced LC posterior displacement, increased curvature, and focal defects is more suggestive of glaucomatous damage, supporting the need for stricter target IOP settings and closer follow-up. Similarly, during longitudinal follow-up, dynamic changes in LC parameters may assist in assessing the relative contributions of different pathological mechanisms to disease progression. In patients with traction-dominant HM, greater emphasis may be placed on long-term structural stability and visual function monitoring, whereas in POAG, progressive LC posterior displacement or thinning may indicate ongoing biomechanical injury and warrant reassessment of treatment efficacy. Therefore, LC-related parameters not only facilitate structural differentiation between diseases but may also contribute to individualized treatment thresholds and optimized follow-up strategies. Integration of LC structural metrics with conventional functional assessments may help establish a more comprehensive risk evaluation framework and form an essential component of future diagnostic models.

Despite these advances, the clinical application of LC assessment remains limited by several factors. One of the most critical challenges is the lack of standardized imaging acquisition and measurement protocols. Variations among OCT or swept-source optical coherence tomography angiography (SS-OCTA) devices in scan patterns, segmentation algorithms, reference plane selection, and parameter definitions can result in substantial inter-study heterogeneity, thereby limiting comparability across studies and centers. In addition, boundary delineation errors in small or tilted optic discs, as well as scaling inaccuracies related to axial length in highly myopic eyes, further compromise measurement accuracy and reproducibility. More importantly, universally validated threshold values for LC-related parameters have not yet been established. Although LCT, LCD, and LCCI are strongly associated with glaucomatous damage, differences in study populations, disease stages, and imaging methodologies make it difficult to define definitive diagnostic cutoffs for direct clinical decision-making. At present, LC parameters are better interpreted as continuous structural markers rather than dichotomous diagnostic indicators.

Future research should focus on several key directions. First, large-scale normative databases across different imaging devices and populations are needed to standardize LC quantitative metrics and explore clinically meaningful diagnostic thresholds. Second, further optimization of deep imaging technologies is required to improve LC visibility and measurement accuracy. Third, integrating LC structural and perfusion parameters with retinal nerve fiber layer thickness, ganglion cell-inner plexiform layer measurements, and visual field-based structure-function models may facilitate the development of multidimensional diagnostic and risk assessment systems. Finally, longitudinal studies are essential to clarify the temporal sequence and interactions of LC changes in POAG and HM, thereby elucidating the stage-specific contributions of compressive stress versus tractional forces. In summary, research on the LC is evolving from pure structural observation toward integrated structural and biomechanical assessment. With increasing precision of quantitative measurements and the expanding spectrum of

disease biomarkers, LC-based evaluation is expected to play an increasingly important role in early screening, risk prediction, and individualized monitoring of POAG and HM, providing a more reliable basis for clinical diagnosis and management strategies.

ACKNOWLEDGEMENTS

Foundations: Supported by Xi'an Medical University "Yi zhen Gene Talent Cultivation Program" Student Research Project (No.2024YZ16); Xi'an Medical University 2024 First Batch of University-Level Research Fund (No.2024DXS03); Shaanxi Provincial Department of Education Young Innovative Team Research Program (No.24JP164); Education Department of Shaanxi Provincial Government for Youth Innovation Team Research Program Project (No.23JP151; No.23JP150); Project of the Scientific Research Capacity Enhancement Program of the Shaanxi Provincial Health Commission (No.2025YF-17).

Conflicts of Interest: Mu QQ, None; **Ge P,** None; **Liu X,** None; **Jia J,** None; **Cui N,** None; **Yang XX,** None; **Zhang RX,** None; **Liu Y,** None; **Zhang YY,** None; **He Y,** None.

REFERENCES

1 Wanichwecharungruang B, Kongthaworn A, Wagner D, *et al*. Comparative study of lamina cribrosa thickness between primary angle-closure and primary open-angle glaucoma. *Clin Ophthalmol* 2021;15:697-705.

2 Kapetanakis VV, Chan MPY, Foster PJ, *et al*. Global variations and time trends in the prevalence of primary open angle glaucoma (POAG): a systematic review and meta-analysis. *Br J Ophthalmol* 2016;100(1):86-93.

3 Pan W, Saw SM, Wong TY, *et al*. Prevalence and temporal trends in myopia and high myopia children in China: a systematic review and meta-analysis with projections from 2020 to 2050. *Lancet Reg Health West Pac* 2025;55:101484.

4 Hamid S, Desai P, Hysi P, *et al*. Population screening for glaucoma in UK: current recommendations and future directions. *Eye (Lond)* 2022;36(3):504-509.

5 Chelvaraj R, Hanapi MS, Mohd-Yusof SF, *et al*. Opportunistic eye screening among first-degree relatives of glaucoma patients at a suburban tertiary center in Malaysia. *Cureus* 2022;14(6):e25772.

6 Chen YH, Hui YN. Commentary review on peripapillary morphological characteristics in high myopia eyes with glaucoma: diagnostic challenges and strategies. *Int J Ophthalmol* 2021;14(4):600-605.

7 Kuang G, Halimitabrizi M, Edziah AA, *et al*. The potential for mitochondrial therapeutics in the treatment of primary open-angle glaucoma: a review. *Front Physiol* 2023;14:1184060.

8 Iwase A, Araie M. Implications of myopia in diagnosis and screening of open angle glaucoma. *Curr Opin Ophthalmol* 2025;36(2):107-114.

9 Yang XY, Xie ST, Wang J, *et al*. Health-related quality of life and its associated factors among high school students with myopia in China. *BMC Public Health* 2025;25(1):3452.

10 Sun MT, Tran M, Singh K, *et al*. Glaucoma and myopia: diagnostic challenges. *Biomolecules* 2023;13(3):562.

11 Tan NYQ, Sng CCA, Jonas JB, *et al*. Glaucoma in myopia: diagnostic dilemmas. *Br J Ophthalmol* 2019;103(10):1347-1355.

12 Fricke TR, Jong M, Naidoo KS, *et al*. Global prevalence of visual impairment associated with myopic macular degeneration and temporal trends from 2000 through 2050: systematic review, meta-analysis and modelling. *Br J Ophthalmol* 2018;102(7):855-862.

13 Liang JH, Pu YQ, Chen JQ, *et al*. Global prevalence, trend and projection of myopia in children and adolescents from 1990 to 2050: a comprehensive systematic review and meta-analysis. *Br J Ophthalmol* 2025;109(3):362-371.

14 Liang JH, Pu YQ, Chen JQ, *et al*. Global prevalence, trend and projection of myopia in children and adolescents from 1990 to 2050: a comprehensive systematic review and meta-analysis. *Br J Ophthalmol* 2025;109(3):362-371.

15 Du Y, Meng JQ, He WW, *et al*. Complications of high myopia: an update from clinical manifestations to underlying mechanisms. *Adv Ophthalmol Pract Res* 2024;4(3):156-163.

16 Wu J, Hao J, Du YF, *et al*. The association between myopia and primary open-angle glaucoma: a systematic review and meta-analysis. *Ophthalmic Res* 2022;65(4):387-397.

17 Tham YC, Aung T, Fan Q, *et al*. Joint effects of intraocular pressure and myopia on risk of primary open-angle glaucoma: the Singapore epidemiology of eye diseases study. *Sci Rep* 2016;6:19320.

18 Elkington AR, Inman CBE, Steart PV, *et al*. The structure of the lamina cribrosa of the human eye: an immunocytochemical and electron microscopical study. *Eye (Lond)* 1990;4(1):42-57.

19 Brazile BL, Yang B, Waxman S, *et al*. Lamina cribrosa capillaries straighten as intraocular pressure increases. *Invest Ophthalmol Vis Sci* 2020;61(12):2.

20 Strickland RG, Garner MA, Gross AK, *et al*. Remodeling of the lamina cribrosa: mechanisms and potential therapeutic approaches for glaucoma. *Int J Mol Sci* 2022;23(15):8068.

21 Kim JA, Lee SH, Son DH, *et al*. Morphologic changes in the lamina cribrosa upon intraocular pressure lowering in patients with normal tension glaucoma. *Invest Ophthalmol Vis Sci* 2022;63(2):23.

22 Jia X, Zhang F, Cao MD, *et al*. Elevated IOP alters the material properties of sclera and lamina cribrosa in monkeys. *Dis Markers* 2022;2022(1):5038847.

23 Hu R, Wu Q, Yi Z, Chen C. Multimodal imaging of optic nerve head abnormalities in high myopia. *Front Neurol* 2024;15:1366593.

24 Lee SH, Kim TW, Lee EJ, *et al*. Ocular and Clinical Characteristics Associated with the Extent of Posterior Lamina Cribrosa Curve in Normal Tension Glaucoma. *Sci Rep* 2018;8(1):961.

25 Wu J, Du YF, Li JY, *et al*. The influence of different intraocular pressure on lamina cribrosa parameters in glaucoma and the relation clinical implication. *Sci Rep* 2021;11:9755.

26 Shin HJ, Costello F. Imaging the optic nerve with optical coherence tomography. *Eye (Lond)* 2024;38(12):2365-2379.

27 Han YX, Wang XF, Xue CC, *et al*. Lamina cribrosa configurations in highly myopic and non-highly myopic eyes: the Beijing eye study. *Invest Ophthalmol Vis Sci* 2024;65(8):28.

28 Lommatzsch C, van Oterendorp C. Current status and future perspectives of optic nerve imaging in glaucoma. *J Clin Med* 2024;13(7):1966.

29 Baskan B, Atas M, Demircan S. Evaluation of lamina cribrosa parameters, nerve fiber thickness, and macular thickness in primary open-angle glaucoma and pseudoexfoliation glaucoma using optical coherence tomography. *Int Ophthalmol* 2024;44(1):378.

30 Tsai YC, Lee HP, Tsung TH, *et al*. Unveiling novel structural biomarkers for the diagnosis of glaucoma. *Biomedicines* 2024;12(6):1211.

31 Lee SM, Park MS, Shin G, *et al*. Lamina cribrosa morphology and clinical implications in glaucoma with thin central corneal thickness. *Sci Rep* 2025;15:22418.

32 Enomoto N, Saito H, Araie M, *et al*. Effect of deep optic nerve head morphology on lamina cribrosa and peripapillary scleral configurations in healthy eyes. *Invest Ophthalmol Vis Sci* 2025;66(9):66.

33 Lee SH, Kim TW, Lee EJ, *et al*. Lamina cribrosa curvature in healthy Korean eyes. *Sci Rep* 2019;9:1756.

34 Ergen A, Yılmaz Tuğan B. Lamina cribrosa curvature depth and index as novel parameters in Graves' ophthalmopathy. *Sci Rep* 2025;15:22981.

35 Ermis S, Ozal E, Arabaci IC, *et al*. Lamina cribrosa curvature index as a biomarker of non-glaucomatous optic neuropathy in obstructive sleep apnea syndrome. *Indian J Ophthalmol* 2025;73(10):1443-1448.

36 Canleblebici M, Celiker U, Yıldırım H, *et al*. Evaluation of lamina cribrosa curvature index in different types of glaucoma. *Int Ophthalmol* 2024;44(1):284.

37 Kong JH, Park SP, Na KI. Differences in optic nerve head structure between acute angle-closure glaucoma and open-angle glaucoma. *Sci Rep* 2023;13:7935.

38 Jeoung JW, Yang HL, Gardiner S, *et al*. Optical coherence tomography optic nerve head morphology in myopia I: implications of anterior scleral canal opening versus bruch membrane opening offset. *Am J Ophthalmol* 2020;218:105-119.

39 Ivers KM, Sredar N, Patel NB, *et al*. *In vivo* changes in lamina cribrosa microarchitecture and optic nerve head structure in early experimental glaucoma. *PLoS One* 2015;10(7):e0134223.

40 Alexopoulos P, Glidai Y, Ghassabi Z, *et al*. Under pressure: lamina cribrosa pore path tortuosity in response to acute pressure modulation. *Trans Vis Sci Tech* 2023;12(4):4.

41 Park SC, Brumm J, Furlanetto RL, *et al*. Lamina cribrosa depth in different stages of glaucoma. *Invest Ophthalmol Vis Sci* 2015;56(3):2059.

42 Lee SH, Kim TW, Lee EJ, *et al*. Diagnostic power of lamina cribrosa depth and curvature in glaucoma. *Invest Ophthalmol Vis Sci* 2017;58(2):755-762.

43 Moghimi S, Nekoozadeh S, Motamed-Gorji N, *et al*. Lamina cribrosa and choroid features and their relationship to stage of pseudoexfoliation glaucoma. *Invest Ophthalmol Vis Sci* 2018;59(13):5355-5365.

44 Esen Baris M, Guven S. Anatomic features of the lamina cribrosa and optic disc in ocular hypertension, glaucoma and healthy eyes. *J Glaucoma* 2024;33(11):823-827.

45 Fernández-Albarral JA, Ramírez AI, de Hoz R, *et al*. Glaucoma: from pathogenic mechanisms to retinal glial cell response to damage. *Front Cell Neurosci* 2024;18:1354569.

46 Sung MS, Heo MY, Heo H, *et al*. Bruch's membrane opening enlargement and its implication on the myopic optic nerve head. *Sci Rep* 2019;9:19564.

47 Burgoyne CF, Wang YX, Jeoung JW, *et al*. OCT optic nerve head morphology in myopia II: peri-neural canal scleral bowing and choroidal thickness in high myopia—an American ophthalmological society thesis. *Am J Ophthalmol* 2023;252:225-252.

48 Xiao D, Lhamo T, Meng Y, *et al*. Peripapillary hyperreflective ovoid mass-like structures: multimodal imaging and associated diseases. *Front Neurol* 2024;15:1379801.

49 Kim YW, Jeoung JW, Kim DW, *et al*. Clinical assessment of lamina cribrosa curvature in eyes with primary open-angle glaucoma. *PLoS One* 2016;11(3):e0150260.

50 Lee S, Heisler M, Ratra D, *et al*. Effects of myopia and glaucoma on the neural canal and lamina cribrosa using optical coherence tomography. *J Glaucoma* 2023;32(1):48-56.

51 Dai JY, Wang XF, Han YX, *et al*. High myopia-induced optic nerve head deformation and glaucoma progression: a three-year follow-up study. *Invest Ophthalmol Vis Sci* 2025;66(13):30.

52 KhalafAllah MT, Fuchs PA, Nugen F, *et al*. Longitudinal changes of bruch's membrane opening, anterior scleral canal opening, and border tissue in experimental juvenile high myopia. *Invest Ophthalmol Vis Sci* 2023;64(4):2.

53 Liu TT, Wang YX, Jonas JB, *et al*. Gaze-induced optic nerve head deformations are greater in high myopia and strains increase with axial length. *Invest Ophthalmol Vis Sci* 2025;66(9):21.

54 Chen YH, Mi BY, Li HR, *et al*. Thinning of the lamina cribrosa and deep layer microvascular dropout in patients with open angle glaucoma and high myopia. *J Glaucoma* 2023;32(7):585-592.

55 Shang X, Häner NU, Lincke JB, *et al*. Long-term changes in lamina cribrosa curvature index after trabeculectomy in glaucomatous eyes. *Invest Ophthalmol Vis Sci* 2024;65(11):3.

56 Englmaier VA, Storp JJ, Leclaire MD, *et al*. Accuracy of Bruch's membrane opening minimum rim width and retinal nerve fiber layer thickness in glaucoma diagnosis depending on optic disc size. *Graefe's Arch Clin Exp Ophthalmol* 2024;262(6):1899-1910.

57 Sun L, Xue M, Tang Y, *et al*. Association of choroidal thickness and blood flow features with asymmetric axial lengths in children with unilateral myopic anisometropia. *BMC Ophthalmol* 2024;24(1):329.

58 Lee EJ, Han DK, Roh YJ, *et al*. Underlying microstructure of the lamina cribrosa at the site of microvasculature dropout. *Invest Ophthalmol Vis Sci* 2024;65(8):47.

59 Paulo A, Vaz PG, Andrade De Jesus D, *et al*. Optical coherence

tomography imaging of the lamina cribrosa: structural biomarkers in nonglaucomatous diseases. *J Ophthalmol* 2021;2021(1):8844614.

60 Zhang YQ, Zhang XJ, Shen RY, *et al*. Exploring optical coherence tomography parameters in eyes with myopic tilted disc. *Eye Vis (Lond)* 2024;11:47.

61 Kudsieh B, Fernández-Vigo JI, Flores-Moreno I, *et al*. Update on the utility of optical coherence tomography in the analysis of the optic nerve head in highly myopic eyes with and without glaucoma. *J Clin Med* 2023;12(7):2592.

62 Nakayama LF, Zago Ribeiro L, de Oliveira JAE, *et al*. Fairness and generalizability of OCT normative databases: a comparative analysis. *Int J Retina Vitreous* 2023;9(1):48.